I&EC research
Industrial & Engineering Chemistry Research

pubs.acs.org/IECR
Article

Regulating the Coordination Mode of Ti Atoms in the Beta Zeolite Framework to Enhance the 1-Hexene Epoxidation

Xuliang Deng,[#] Yang Xu,[#] Jincheng Liu,[#] Dong Lin,[*] Ze Zong, Juncong Yuan, Zhiyang Li, Guanghui Zhao, Yongjun Zhang, Yibin Liu, Xiaobo Chen, Xiang Feng,[*] De Chen, Chaohe Yang,[*] and Honghong Shan

Cite This: https://doi.org/10.1021/acs.iecr.3c03543

ABSTRACT: Regulating the Ti active sites in titanosilicates with different coordination modes is of prime scientific and industrial significance to the rational design of efficient catalysts for olefin epoxidation. In this study, the Ti species in Ti-beta zeolite catalysts (open/closed tetra-coordinated Ti sites, hexa-coordinated Ti species, and TiO_2) were keenly controlled via the dealumination-metallization approach. By multiple characterizations, kinetics study, and multivariate model analysis, it is found that the open tetra-coordinated framework $Ti(OH)(OSi)_3$ species contribute more to the catalytic performance for 1-hexene epoxidation with H_2O_2. Moreover, the Ti-beta with rich open tetra-coordinated $Ti(OH)(OSi)_3$ species showed significantly improved reaction performance (TON: 401, conversion: 64%, selectivity: 98%, H_2O_2 efficiency: 97%) with lower apparent activation energy. This study not only opens up new prospects for the design of efficient titanosilicates by modifying Ti microenvironments but also proposes the strategy to improve the content of open tetra-coordinated Ti sites.

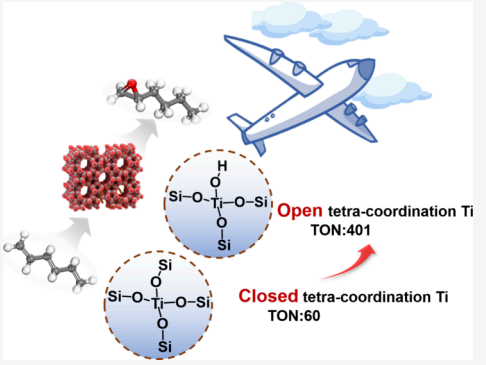

1. INTRODUCTION

1,2-Epoxyhexane is a crucial oxygen-containing derivative of 1-hexene, serving as the raw material for value-added chemical products like cosmetic additives, polyester fibers, and pharmaceutical intermediates.[1,2] 1,2-Hexanediol, as the hydrolysis product of 1,2-epoxyhexane, is an important pharmaceutical intermediate with high global consumption and high cost, and the demand has been increasing year by year.[3−6] Considering the importance of 1,2-epoxyhexane, the need to develop value-added C_6 products (i.e., 1,2-epoxyhexane) is urgent.[7] Divergent compounds such as organometallic and inorganic metal oxides have been employed as catalysts for 1-hexene epoxidations utilizing various oxidants, e.g., oxygen, ozone, and hydrogen peroxide or organic peroxides.[8,9] However, most of epoxidation processes (i.e., chlorohydrin process and *tert*-butyl hydroperoxide process) require complicated production processes and huge capital investment.[10,11] In particular, the method utilizing hydrogen peroxide (H_2O_2) as an oxidizing agent has the advantages of environmental friendliness, mild reaction conditions, and a high reactive oxygen content. It has attracted worldwide attention as a promising epoxidation method for industrialization.[12,13]

In olefin epoxidation, the first generation of titanosilicate (i.e., titanium silicalite-1) was introduced by Taramasso in 1983,[14] which later proved to be an efficient and environmentally friendly catalyst for selective oxidation reactions using H_2O_2 as an oxidant.[15−17] For TS-1, it is generally believed that the tetra-coordinated Ti species[18] (i.e., "open" and "closed" tetra-coordinated Ti species) and hexa-coordinated Ti species[19−22] are both active for olefin epoxidation. Some works show that the "open" tetra-coordinated Ti species ($Ti(OH)(OSi)_3$) with Ti−OH are more active than the $Ti(OSi)_4$ species due to the presence of strong Lewis acids[23,24] for propene epoxidation reaction. In contrast, some recent studies also suggested that hexa-coordinated Ti species are also important active sites for 1-hexene epoxidation.[24,25] However, there is still no work on systematically elucidating the intrinsic Ti active sites for 1-hexene epoxidation by keenly controlling different Ti species (i.e., open/closed tetra-coordinated Ti and hexa-coordinated Ti).[26] The relationship between Ti species and catalytic performance is highly desired for the design of efficient catalysts for hexene epoxidation.[27−29]

In this study, the coordination mode of Ti species (i.e., open/closed tetra-coordinated Ti, hexa-coordinated Ti, and also TiO_2) was controlled and the intrinsic active sites were elucidated for 1-hexene epoxidation. By multiple character-

Received: October 8, 2023
Revised: February 5, 2024
Accepted: February 13, 2024

izations, kinetics study, and multivariate model analysis, it is found that the open tetra-coordinated framework Ti species ($Ti(OH)(OSi)_3$ species) are more efficient than closed tetra-coordinated framework Ti species, hexa-coordinated Ti species, and TiO_2 species in 1-hexene epoxidation. The Ti-beta catalysts with rich open tetra-coordinated Ti species exhibit significantly improved reaction performance (TON: 401, conversion: 64%, selectivity: 98%, H_2O_2 efficiency: 97%) due to the lower apparent activation energy. This study not only sheds light on the underlying mechanism of 1-hexene epoxidation but also paves the way for the design of highly efficient titanosilicate.

2. EXPERIMENTAL SECTION

2.1. Dealumination-Metallization Process of Ti-Beta. Ti-beta zeolites were synthesized using a dealumination-metallization strategy, effectively overcoming challenges related to temperature-induced structural deviations and disparate hydrolysis rates between Ti and Si species.[30,31] In this study, 10 g of pristine Al-beta zeolite (SiO_2/Al_2O_3 = 25, provided by Nankai Catalyst Plant) underwent treatment with 250 mL of a 13 mol·L^{-1} aqueous HNO_3 solution (Sinopharm Chemical Reagent Co., Ltd.) in a 500 mL three-neck flask equipped with a reflux condenser. The mixture was maintained at 100 °C for 24 h, resulting in the removal of the framework aluminum. After post-HNO_3 treatment, the remaining Al content was less than 0.1% based on ICP analysis, indicating successful aluminum removal. The resulting solid underwent thorough washing with deionized water, followed by drying at 110 °C for 2 h and calcination at 550 °C for 3 h, resulting in the formation of nested silanol sites. During Ti incorporation, an appropriate quantity of $TiCl_4$ (99.9%, Macklin) was reacted with anhydrous ethanol. Subsequently, 2 g of H-beta was mixed with 10 mL of the Ti precursor and the mixture was further stirred. The final products were collected, dried at 100 °C for 2 h, and subjected to calcination at 550 °C for 3 h. These samples were named as *m*% Ti-beta-post, where *m* represents the Ti content in the samples.

2.2. Characterizations. The crystal structure of the Ti-beta sample was measured using X-ray diffraction (XRD, X'Pert PRO MPD, Cu K_α radiation). The scanning speed of the XRD was 10°/min. The relative crystallinity was determined by comparing the peak area at 2θ = 7.8, 14.5°, 22.5, and 27.1° to that of the Al-beta catalyst. The determination of Ti species in TS-beta was carried out using an ultraviolet−visible method (UV−vis, Shimadzu UV-2700) after drying on the ovens, and pure $BaSO_4$ was used as the background. The relative percentage of framework Ti species in all Ti species was calculated based on the Gaussian fitting method (four Gaussian profiles: tetracoordination Ti at 200 nm, open tetracoordination Ti at 220−235 nm, hexagonal Ti at 270 nm, and anatase TiO_2 species at 330 nm). Moreover, the multivariate fitting was carried out using least squares. The R^2 of the fitting results is beyond 0.99. The values (blue) calculated from the multivariate fitting model are in agreement with the experimental values (red) in Figure 5. The Ti content of the samples was determined using Agilent 730 inductively coupled plasma emission spectrometry (ICP-OES). The Lewis and Brønsted acid sites in Ti-beta-post catalysts were characterized by the infrared (IR) spectra of adsorbed pyridine (Macklin, >99%). The custom-built transmission cell was coupled to a Fourier transform infrared (FTIR) spectrometer (Nicolet NEXUS 670) with a liquid-N_2-cooled detector. Catalysts were pressed into self-supporting disks (20 mg) and placed within the transmission cell, which was assembled by using KBr windows and connected to a gas three-way valve. All materials were first heated to 500 °C at 10 °C·min^{-1} and held for 1 h under flowing air to desorb water and residual organics. Pyridine was introduced via a syringe pump three-way valve for 45 min to adsorb pyridine entirely at 25 °C. The physisorbed and chemisorbed pyridines were then removed by evacuation at 200 °C for 0.5 h. The FTIR of the hydroxyl stretching region was recorded in the region between 2500 and 4000 cm^{-1}. The spectra in the hydroxyl stretching region were collected at ambient temperature after the treatment at 500 °C for 2 h under vacuum conditions. The FTIR spectra in the framework vibration region of the titanosilicates were recorded at 25 °C.

2.3. Catalytic Testing. The as-synthesized Ti-beta zeolite was tested in 1-hexene epoxidation. All reactions were performed in a 50 mL microreactor at a temperature of 25 °C. Reaction conditions were as follows: 0.2 g of catalyst, 1.2 g of 1-hexene (AR, Aladdin), 1.2 g H_2O_2 (>30 wt %, Sinopharm Chemical Reagent Co., Ltd.), and 20 mL of CH_3CN (AR, Sinopharm Chemical Reagent Co., Ltd.). The reaction temperature was maintained at 60 °C, and the reaction time was 3 h, according to previous studies.[32,33] The resultant solution was transferred to a transparent sample vial containing anhydrous sodium sulfate and homogeneously mixed to remove any residual water. The supernatant was then collected, and 1 mL of the sample was taken under continuous stirring and transferred to a chromatographic vial for subsequent analysis. H_2O_2 utilization was confirmed by the iodometric method. The procedure for activating the Ti-beta-post with H_2O_2 is as follows: After 12 h of drying, 5 mL of H_2O_2 is meticulously mixed with the Ti-beta-post catalysts, followed by centrifugation to yield the H_2O_2-activated catalyst.

The reaction products were quantified by gas chromatography (Agilent 7820A with an autosampler and HP-530 M 320 × 0.25 μm) and an FID detector. The substrate conversion, product yield, and selectivity were determined according to the standard curves of the corresponding materials. Gas chromatography used high-purity nitrogen as carrier gas and an inlet and detector temperature of 280 °C. The column temperature program was maintained at 60 °C for 2 min, followed by a 20 °C·min^{-1} ramp-up to 230 °C and then from 230 to 280 °C (ramp-up rate of 5 °C·min^{-1}), and maintained at 280 °C for 5 min.

The iodometric method was employed for the quantitative analysis of H_2O_2 in the present study: ca. 0.30 g of prereaction and postreaction solutions was accurately weighed in an iodometric flask, and 20 wt % H_2SO_4 solution was added to the flask. Subsequently, saturated ammonium molybdate solution was dropwise added (approximately 1 mL), followed by the addition of 2 mL of 10 wt % KI solution after proper shaking. The piston was covered, and the flask was sealed in a light-proof environment for 20 min. Subsequently, the 0.1 mol L^{-1} sodium thiosulfate ($Na_2S_2O_3$) solution was prepared and transferred into an alkaline buret. The previously prepared solution was taken out. A calibrated solution of sodium thiosulfate was then carefully dripped into the solution until it discolored; then, approximately 2 mL of starch solution was added dropwise as an indicator, indicating the completion of titration. The chemical reactions involved in this process are as follows:

https://doi.org/10.1021/acs.iecr.3c03543
Ind. Eng. Chem. Res. XXXX, XXX, XXX−XXX

$$H_2O_2 + 2I^- + 2H^+ \rightarrow I_2 + 2H_2O \quad (2\text{-}1)$$

$$I_2 + 2Na_2S_2O_3 \rightarrow 2NaI + Na_2S_4O_6 \quad (2\text{-}2)$$

The area of 1-hexene, 1,2-epoxyhexane, and *n*-pentanal was integrated analytically to calculate the reactant conversion and product selectivity, and the conversion of raw material 1-hexene and the selectivity of different products was calculated as follows:

$$C(\%) = \frac{n_0 - n_0'}{n_0} \times 100\% \quad (2\text{-}3)$$

$$S(\%) = \frac{n_1}{n_0' + \sum_1^3 n_i} \times 100\% \quad (2\text{-}4)$$

$$\mathrm{TON} = \frac{n_I}{n_{\mathrm{Ti}}} \quad (2\text{-}5)$$

where C is the conversion of 1-hexene, S is the selectivity of each component in the product, n_0 is the initial molar amount of 1-hexene, n' is the molar amount of 1-hexene remaining in the solution at the end of the reaction, n_1 is the molar amount of 1,2-epoxyhexane, and n_i is the molar amount of a component in the product, and n_{Ti} is the molar amount of the Ti contained in the catalysts.

The titration results were analyzed, where the H_2O_2 concentration was calculated as follows:

$$H_2O_2(\mathrm{wt}\%) = \frac{34.016 \times C_0 \times V_0}{2 \times W \times 1000} \times 100\% \quad (2\text{-}6)$$

where C_0 is the molar concentration of sodium thiosulfate solution, V_0 is the volume of sodium thiosulfate solution consumed, and W is the mass of the weighed sample.

The conversion of H_2O_2 and the effective utilization rate were calculated as follows:

$$X_{H_2O_2}(\%) = \frac{n^0_{H_2O_2} - n'_{H_2O_2}}{n^0_{H_2O_2}} \times 100\% \quad (2\text{-}7)$$

$$\mathrm{Eff.}\ (H_2O_2)(\%) = \frac{X_{H_2O_2}(\%)}{C(\%)} \times 100\% \quad (2\text{-}8)$$

where $n^0_{H_2O_2}$ is the initial molar concentration of H_2O_2, $n'_{H_2O_2}$ is the molar concentration of the remaining H_2O_2, and X is the conversion rate of 1-hexene.

3. RESULTS AND DISCUSSION

3.1. Regulation of Ti Species in the Beta Zeolite Framework. Different Ti species (i.e., TiO_4, $Ti(OH)(H_2O)_{(2)}(OSi)_3$, and anatase TiO_2) are regulated by adjusting the Ti contents in Ti-beta catalysts by the dealumination-metallization approach (Figure 1a). The aluminum beta zeolite (Al-beta) is treated with nitric acid to remove the framework aluminum species, creating silanol defects (vacant T sites) in the beta zeolite framework.

These Ti precursors subsequently undergo a reaction with the silanol groups, leading to further anchoring of Ti atoms at the T sites. This process results in the formation of isolated framework Ti species, namely, open/closed tetra-coordinated TiO_4 and hexa-coordinated $Ti(OH)(H_2O)_{(2)}(OSi)_3$. With the increase of the total Ti content, the relative content of different Ti species can be regulated. The total Ti content of the Ti-beta catalysts was determined by ICP-OES analysis and are presented in Table S1. These results show that the Ti content is gradually increased from 0.45 to 3.1 wt %.

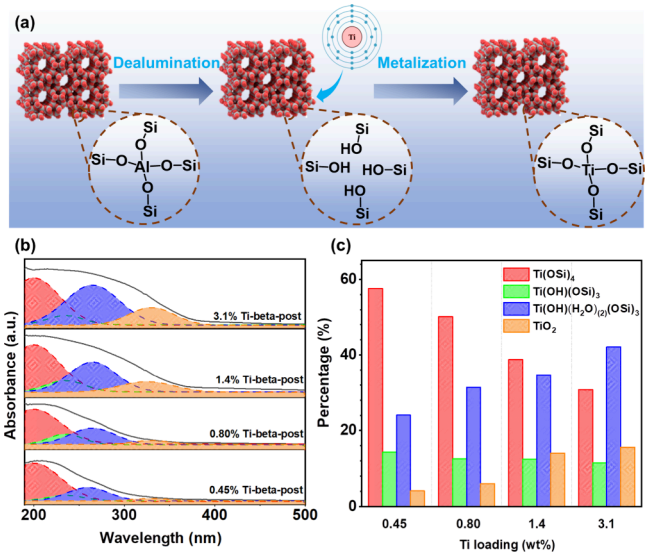

Figure 1. (a) The synthetic mechanism of Ti-beta by the dealumination-metallization process. (b) The UV spectra of Ti-beta with different Ti contents: 0.45% Ti-beta-post, 0.80% Ti-beta-post, 1.4%Ti-beta-post, and 3.1% Ti-beta-post. (c) The contents of different Ti species in different Ti-beta samples.

UV−vis spectroscopy is considered as a sensitive method for characterizing the coordination states of Ti species in titanosilicate.[34] The band centered at 200 nm is attributed to the charge transfer from O^{2-} to Ti^{4+} in isolated $Ti(OSi)_4$, while the band ranging from 220 to 235 nm corresponds to the $Ti(OSi)_3(OH)$ species. Both open and closed tetra-coordinated Ti sites were consistently observed in all Ti-beta catalysts.[35] This indicates that some Ti species are tetra-coordinated in the beta zeolite framework.[36] Furthermore, in Ti-beta catalysts, an absorption band around 270 nm emerges, commonly associated with the formation of hexa-coordinated Ti species.[37] Additionally, a prominent absorption band at approximately 330 nm is evident in the Ti-beta catalysts, indicative of the presence of anatase TiO_2.[36,37] It is found that with the increase of Ti contents in the Ti-beta catalysts from 0.45 to 3.1 wt %, the percentage of closed tetra-coordinated Ti species gradually decreases from 57.55 to 30.76%, and the percentage of open tetra-coordinated Ti species also decreases from 14.30 to 11.47% (Figure 1c). However, the relative proportion for hexa-coordinated Ti species gradually increase from 24.06 to 42.15% and the relative proportion for anatase TiO_2 species also increase from 4.09 to 15.61% (Figure 1c). The content of hexa-coordinated Ti species and anatase TiO_2 species gradually increased, while the content of closed tetra-coordinated Ti species and open tetra-coordinated Ti species gradually decreased. The diverse growth directions and rates demonstrated that the distribution of Ti species was controlled by regulating Ti contents during the dealumination-metallization approach.

The physicochemical properties of Ti-beta catalysts are further examined. The XRD patterns of the four samples (Figure 2a) show similar diffraction peaks located at 2θ = 7.8, 14.5, 22.5, and 27.1°, which confirm the beta zeolite topological structure of four Ti-beta catalysts.[38] After the incorporation of the Ti atom, there is a slight shift for the diffraction peak from 22.6 to 22.5° with the increase of Ti

https://doi.org/10.1021/acs.iecr.3c03543
Ind. Eng. Chem. Res. XXXX, XXX, XXX−XXX

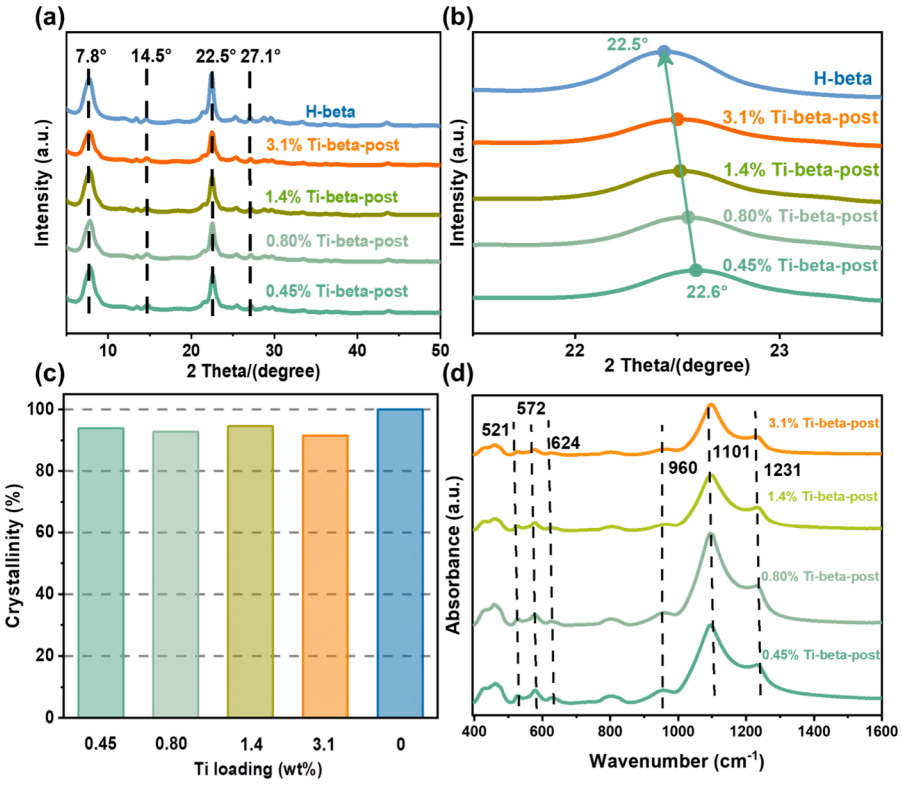

Figure 2. (a) XRD patterns of Ti-beta-post catalysts with different Ti contents. (b) XRD patterns for shift from 22.5 to 22.6° for different Ti-beta-post catalysts. (c) The relative crystallinity of different Ti-beta-post catalysts. (d) FTIR spectra of Ti-beta-post catalysts.

contents (Figure 2b). Because Ti atoms are larger in size compared to Al atoms, their incorporation into the zeolite framework can lead to the expansion of the framework. The larger Ti atoms result in an increased unit cell size, consequently reducing the 2θ values of XRD reflections.[39] Figure 2c was used to show the crystallinity of different Ti-beta-post catalysts. The results show that the beta zeolite frameworks of different Ti-beta-post catalysts are all damaged to some extent due to the decreased crystallinity compared with the parent Ti-beta.

As shown in Figure 2d, all of the FTIR spectra of four catalysts show two characteristic bands at 1101 and 1231 cm^{-1}, which are associated with the T−O asymmetric stretch of internal linkages and external linkages in the beta zeolite,[40−42] respectively. The observed peaks at 521, 572, and 624 cm^{-1} in the FTIR spectra are attributed to the stretching vibration of double rings and [SiO_4] units in the beta zeolite framework.[36] Additionally, the presence of the band at 960 cm^{-1} is commonly considered as the proof for the incorporation of Ti atoms in the zeolite framework,[38,43] indicating that the Ti atoms were well incorporated into the beta zeolite framework during the metallization process.

In order to further verify the effects of the dealumination-metallization approach on the acid sites of the Ti-beta catalysts, different characterizations such as NH_3-TPD, infrared (IR) spectra of pyridine adsorption, and FTIR spectra in the hydroxyl stretching region of Ti-beta-post catalysts are further performed (Figure 3). First, it can be seen that only one obvious NH_3 desorption peak of Ti-beta catalysts appears at 139 °C (Figure 3a), which is ascribed to weak acid centers.[44,45] Moreover, with the incorporation of Ti atoms into the framework, there is a slight shift for the NH_3 desorption peak from 139 to 142 °C. This slight shift should be attributed to the gradually increased weak acid sites due to the significant increase of TiO_2 content.[46]

In addition, the number of surface acid sites of the four catalysts follows the order 3.1 wt %Ti-beta-post (0.138 mmol/g) > 1.4 wt %Ti-beta-post (0.131 mmol/g) > 0.80 wt %Ti-beta-post (0.096 mmol/g) > 0.45 wt %Ti-beta-post (0.076 mmol/g), and the shift for the NH_3 desorption peak also follows this order. Obviously, more strong acid sites were formed as the TiO_2 content increases. Therefore, there might be a correlation between the nonframework TiO_2 and the acidity.[47] The ratio of the Brønsted/Lewis acidity of the catalysts was further investigated by the IR spectra of pyridine adsorption (Figure 3c,d). The ratio of Brønsted/Lewis acidity sites gradually decreases with the increase in Ti content (Figure 3d). It means that nonframework TiO_2 provide more and stronger Lewis acidity than the Brønsted acidity formed by the open tetra-coordinated TiO_4 and hexa-coordinated TiO_6.[48] The presence of excessively strong Lewis acids in TiO_2, characterized by an abundance of surface acid sites, results in the inefficient decomposition of H_2O_2. This observation of increased TiO_2 contents is consistent with the findings illustrated in the UV−vis spectra (Figure 1c).

The FTIR spectra in the hydroxyl stretching region are collected to characterize the microenvironment of different Ti-beta catalysts synthesized with different percentages of Ti species (Figure 3e). All the catalysts show the band around 3740 cm^{-1}, which is ascribed to the isolated external silanol group.[49] Moreover, the four catalysts have a wide band at 3540 cm^{-1}, indicating the appearance of the hydrogen-bonded silanol group on defect sites such as hydroxyl nests resulting from the dealumination.[50] The characteristic band at 3540 cm^{-1} indicates the presence of a cluster of hydroxyl groups tightly bound by hydrogen bonds.[49] In addition, the band at

https://doi.org/10.1021/acs.iecr.3c03543
Ind. Eng. Chem. Res. XXXX, XXX, XXX−XXX

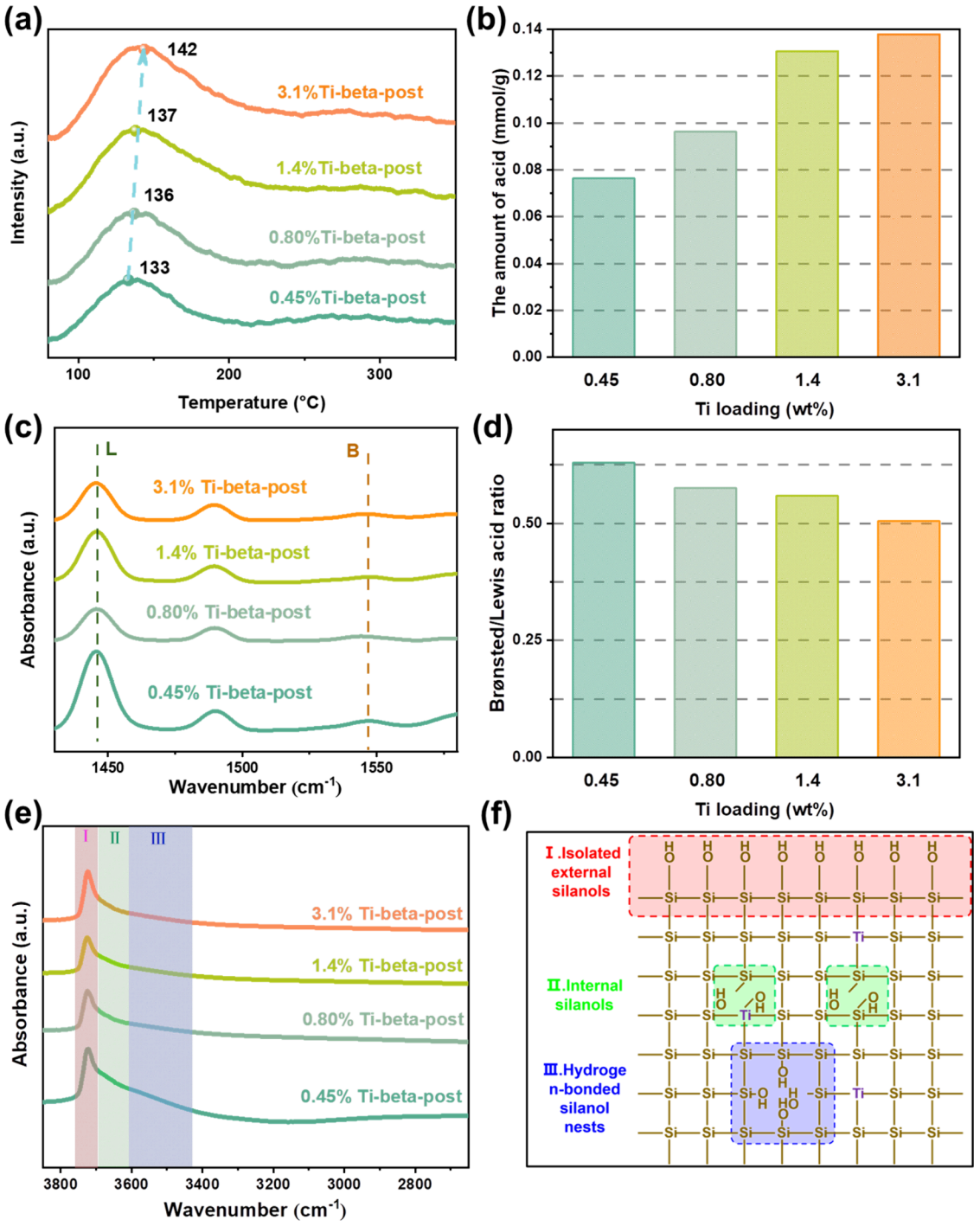

Figure 3. (a) NH_3-TPD spectra of different Ti-beta-post catalysts. (b) The amount of acid sites in different Ti-beta-post catalysts. (c) The IR spectra of pyridine adsorption of different Ti-beta-post catalysts. (d) The Brønsted/Lewis acid ratio of different Ti-beta catalysts. (e) FTIR spectra in the hydroxyl stretching region evaluated at 723 K in the range of 2600−4000 cm^{-1} of different Ti-beta-post catalysts. (f) The schematic diagram of different silanol groups in Ti-beta-post catalysts.

3697 cm^{-1} is related to the internal silanol group.[51] With the increase of Ti content, the band intensity at 3540 and 3697 cm^{-1} gradually decreases, implying that more Ti species are incorporated into vacancies. This suggests a structure change in Ti-beta-post catalysts, which can be expressed as follows:[52,53]

$$Ti - OH + Si - OH = Si - O - Ti + H_2O$$

These results indicated that as the Ti content in Ti-beta-post catalysts increases, the hydrogen-bonded silanol groups and internal silanols react with Ti species. Subsequently, the silanol defects (vacant T sites) are filled with Ti atoms, effectively repairing the surface of vacant T sites.

3.2. Active Sites for the 1-Hexene Epoxidation. In order to investigate the Ti active sites in the epoxidation system of 1-hexene/H_2O_2, the relationship between the TON and percentages of different Ti species is shown in Figure 4. It

https://doi.org/10.1021/acs.iecr.3c03543
Ind. Eng. Chem. Res. XXXX, XXX, XXX−XXX

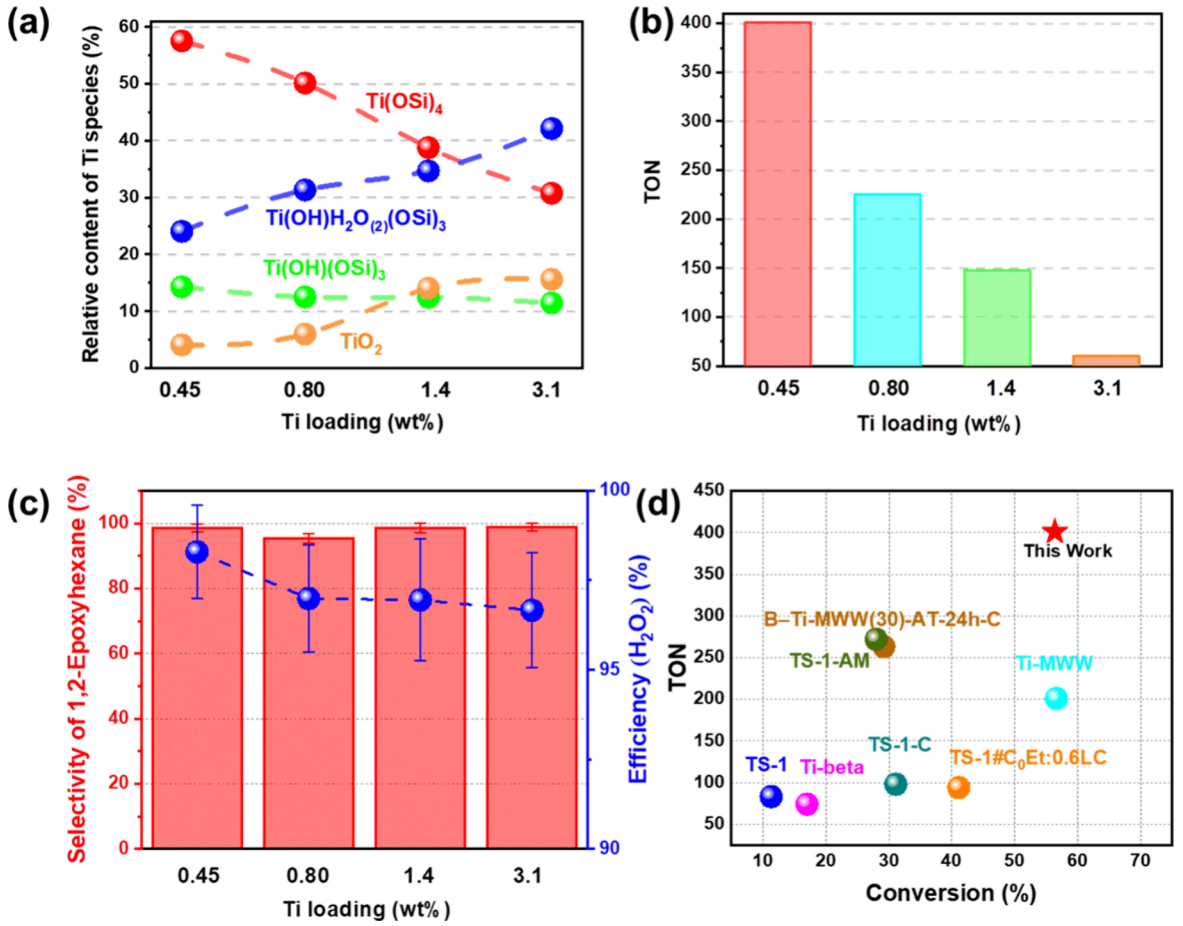

Figure 4. (a) The relative content of different Ti species (i.e., $Ti(OSi)_4$, $Ti(OH)(OSi)_3$, $Ti(OH)H_2O_{(2)}(OSi)_3$, and TiO_2) in different catalysts. (b) The TON of 1-hexene epoxidation for different Ti-beta-post catalysts. (c) The selectivity of 1,2-epoxyhexane (red) and utilization efficiency of H_2O_2 (blue) in different catalysts. (d) TON of different catalysts in literature for 1-hexene epoxidation.

is found that as the Ti content increases, the dominant Ti species gradually change from tetra-coordinated Ti species to hexa-coordinated Ti species and further anatase TiO_2 species (Figure 4a). The percentage of closed tetra-coordinated Ti species decreases from 57.55 to 30.76%, and the percentage of open tetra-coordinated Ti species decreases from 14.30 to 11.47%. However, the relative proportion of hexa-coordinated Ti species gradually increases from 24.06 to 42.15% and the relative proportion for anatase TiO_2 species also increases from 4.09 to 15.61%.

In Figure 4b, the TON gradually decreases from 401 to 60 with the increase of Ti content. Moreover, the four distinct Ti-beta-post catalysts consistently demonstrate high and comparable reaction selectivity, as illustrated in Figure 4c (~96%). The minimal presence of byproducts, such as 1-pentanal and 1,2-hexanediol, in the 1-hexene epoxidation can be attributed to the hydrolysis and subsequent deep oxidation of 1,2-epoxyhexane. Notably, the use of an acetonitrile solvent proves effective in suppressing hydrolysis and further deep oxidation reactions, given the lower nucleophilic ability inherent in aprotic solvents like acetonitrile. Consequently, all four Ti-beta-post catalysts exhibit a high selectivity (~96%) for 1,2-epoxyhexane in the 1-hexene epoxidation with H_2O_2. However, with the increase of TiO_2 content, the H_2O_2 average utilization efficiency gradually decreases from 98.29 to 96.66% due to the decomposition of H_2O_2 by anatase TiO_2[54,55] (Figure 4c). Moreover, it should be noted that the 0.45 wt % Ti-beta-post with the highest percentage of tetra-coordinated Ti species shows outstanding epoxidation performance of 1-hexene (TON: 401, selectivity: 98.63%, utilization efficiency of H_2O_2: 98.29%) compared with the results in literatures[25,26,56−60] (Figure 4d).

In order to further verify the multirelationships between Ti content of different Ti species and TON, a multivariate fitting model was conducted, illustrating the correlations among the contents of different Ti species (closed tetra-coordinated Ti species, x_1; open tetra-coordinated Ti species, x_2; hexa-coordinated Ti species, x_3) and TON, as shown in Figure 5a. *a*, *b*, and *c* are coefficients of closed tetra-coordinated Ti species (x_1), open tetra-coordinated Ti species (x_2), and hexa-coordinated Ti species (x_3), respectively. It is found that *b* (35.89) > *a* (22.14) > *c* (−10.33). The highest value of *b* further demonstrates the strong positive correlation between the open tetra-coordinated Ti species and TON. In contrast, the lower values of *a* showed the weaker correlation between the TON and content of closed tetra-coordinated Ti species. A negative coefficient *c* indicates a significantly reduced correlation of hexa-coordinated Ti species with TON. This indicated that the open tetra-coordinated Ti species are major active sites in Ti-beta for 1-hexene epoxidation.

Both open and closed tetra-coordinated TiO_4 sites demonstrate a positive relationship between their contents and TON (Figure 5b,c). Nevertheless, a more robust positive linear correlation is evident between open tetra-coordinated

https://doi.org/10.1021/acs.iecr.3c03543
Ind. Eng. Chem. Res. XXXX, XXX, XXX−XXX

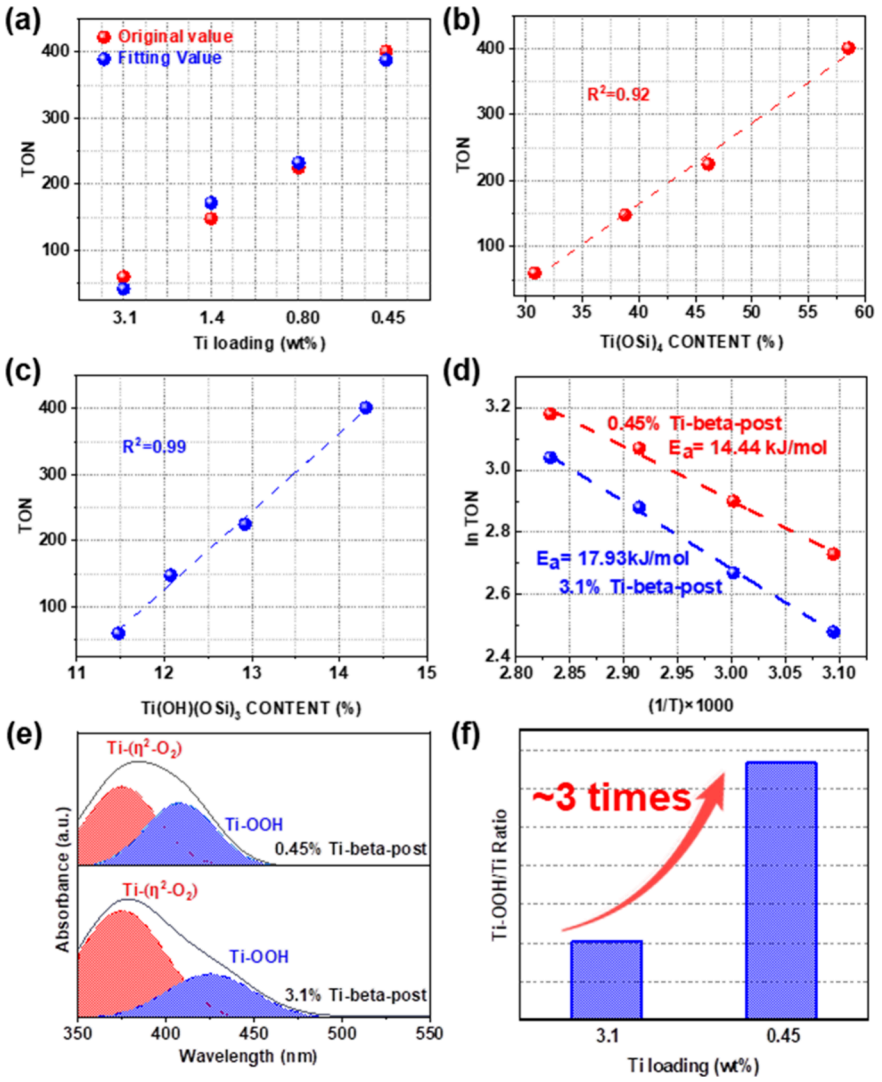

Figure 5. (a) The multivariate fitting for TON and the multi-Ti species (red points: original value, blue points: fitting value). (b) The relationship between TON and the content of closed tetra-coordinated Ti species. (c) The correlation between TON and the open tetra-coordinated Ti species. (d) Plots of apparent activation energy in the 1-hexene epoxidation catalyzed by Ti-beta-post. (e) UV−vis spectra of H_2O_2-activated Ti-beta-post. (f) The different Ti-OOH/Ti contents between the 0.45 and 3.1 wt % Ti-beta-post.

framework Ti species and TON. This underscores that open $Ti(OH)(OSi)_3$ stands out as the predominant active site for 1-hexene epoxidation when compared to closed $Ti(OSi)_4$ species. Therefore, the presence of rich $Ti(OH)(OSi)_3$ in the synthesized Ti-beta-post catalysts should account for this superior reaction performance.

In the kinetics study, the apparent activation energies for 0.45% Ti-beta-post and 3.1% Ti-beta-post were calculated by using the Arrhenius equation for 1-hexene epoxidation (Figure 5d). The obtained values were 14.44 and 17.93 kJ mol^{-1}, respectively. This implies that an increase in the concentration of Ti−OH species corresponds to a decrease in the apparent activation energy (Figure 5d), which could account for the outstanding performance of 1-hexene epoxidation.

Ti-OOH intermediates are commonly regarded as the reactive intermediates on Ti-based heterogeneous catalysts for alkene epoxidation.[26,61] Ti-OOH could be formed after the reaction between active Ti species and H_2O_2.[62] The UV−vis spectra of H_2O_2-activated Ti-beta-post are shown in Figure 5e,f.[63,64] Both Ti-OOH and Ti-(η^2-O_2) were observed on two Ti-beta-post catalysts (0.45% Ti-beta-post and 3.1% Ti-beta-post). The bands at ca. 375 and 425 nm were attributed to Ti-(η^2-O_2) and Ti-OOH,[64−66] respectively. The 0.45% Ti-beta-post shows a three times higher relative ratio (Ti-OOH/Ti content) than that of 3.1% Ti-beta-post (13.33 > 4.06). The higher content of reactive intermediates further demonstrates the higher reaction activity for 1-hexene epoxidation for 0.45% Ti-beta-post.

Therefore, the reaction pathway for the epoxidation of 1-hexene on $Ti(OH)(OSi)_3$ sites is illustrated in Figure 6. In Ti-beta catalysts, the abundance of open $Ti(OH)(OSi)_3$ sites facilitates the easy formation of Ti-η^1(OOH) species (Ti-OOH/Ti ratio: 13.3) compared to other Ti species. This initiation takes place through the reaction between Ti−OH and H_2O_2, demonstrating a remarkably high H_2O_2 average utilization efficiency of 98.29%.[33,67,68] These Ti-η^1(OOH) species are recognized as the active intermediates in olefin epoxidation.[69,70] Subsequently, these active intermediates attack the double bond of 1-hexene via an oxygen atom, leading to the creation of a transition state with a lower apparent activation energy (14.44 kJ mol^{-1}) and the subsequent formation of 1,2-epoxyhexane.[71] Due to their

https://doi.org/10.1021/acs.iecr.3c03543
Ind. Eng. Chem. Res. XXXX, XXX, XXX−XXX

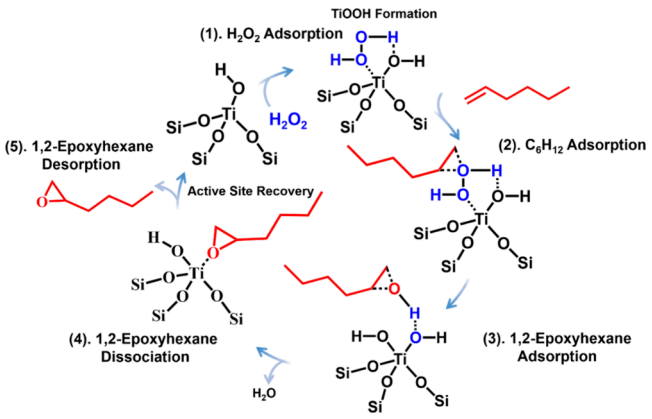

Figure 6. Proposed reaction mechanism of 1-hexene epoxidation on the open tetra-coordinated Ti site of Ti-beta.

ability to activate H_2O_2 into Ti-η^1(OOH) species and lower apparent activation energies, Ti(OH)$(OSi)_3$ sites exhibit superior performance in the epoxidation of 1-hexene.

4. CONCLUSIONS

In summary, the coordination mode of Ti sites within the beta zeolite framework was regulated by the dealumination-metallization approach. It is found that with the increase of Ti content, the percentage of open/closed tetra-coordinated Ti species (e.g., Ti(OH)$(OSi)_3$ and Ti$(OSi)_4$) gradually decrease and the percentages of hexa-coordinated Ti species and TiO_2 species gradually increase. The multiple characterizations, kinetics study, and multivariate model analysis clearly reveal that the open Ti(OH)$(OSi)_3$ species contribute more to the catalytic performance compared with other three Ti species. The Ti-beta catalyst with Ti loading of 0.45% has rich open tetra-coordinated Ti species (Ti(OH)$(OSi)_3$) and shows significantly improved performance. This is attributed to lower apparent activation energies (14.4 kJ mol^{-1}) and a higher ratio of key reaction intermediates (Ti-OOH/Ti, 13.33). This study not only elucidates the fundamental mechanism of 1-hexene epoxidation but also establishes a pathway for the regulation and construction of high-efficient Ti species in titanosilicate.

■ ASSOCIATED CONTENT

Supporting Information

The Supporting Information is available free of charge at https://pubs.acs.org/doi/10.1021/acs.iecr.3c03543.

Ti loading; conversion of 1-hexene; nitrogen adsorption−desorption isotherm; and typical TEM images of 0.45% Ti-beta-post, 0.80% Ti-beta-post, 1.4%Ti-beta-post, and 3.1% Ti-beta-post catalysts (PDF)

■ AUTHOR INFORMATION

Corresponding Authors

Dong Lin − *Max Planck-Cardiff Centre on the Fundamentals of Heterogeneous Catalysis FUNCAT, Cardiff Catalysis Institute, School of Chemistry, Cardiff University, Cardiff CF103AT, United Kingdom;* orcid.org/0000-0001-5313-8204; Email: LinD6@cardiff.ac.uk

Xiang Feng − *State Key Laboratory of Heavy Oil Processing, China University of Petroleum, Qingdao 266580, China;* orcid.org/0000-0001-7299-5690; Email: xiangfeng@upc.edu.cn

Chaohe Yang − *State Key Laboratory of Heavy Oil Processing, China University of Petroleum, Qingdao 266580, China;* orcid.org/0000-0001-6995-9170; Email: yangch@upc.edu.cn

Authors

Xuliang Deng − *State Key Laboratory of Heavy Oil Processing, China University of Petroleum, Qingdao 266580, China; Daqing Chemical Research Center, PetroChina Petrochemical Research Institute, CNPC, Daqing City 163000, China*

Yang Xu − *State Key Laboratory of Heavy Oil Processing, China University of Petroleum, Qingdao 266580, China*

Jincheng Liu − *Daqing Chemical Research Center, PetroChina Petrochemical Research Institute, CNPC, Daqing City 163000, China*

Ze Zong − *State Key Laboratory of Heavy Oil Processing, China University of Petroleum, Qingdao 266580, China*

Juncong Yuan − *State Key Laboratory of Heavy Oil Processing, China University of Petroleum, Qingdao 266580, China*

Zhiyang Li − *State Key Laboratory of Heavy Oil Processing, China University of Petroleum, Qingdao 266580, China*

Guanghui Zhao − *Daqing Chemical Research Center, PetroChina Petrochemical Research Institute, CNPC, Daqing City 163000, China*

Yongjun Zhang − *Daqing Chemical Research Center, PetroChina Petrochemical Research Institute, CNPC, Daqing City 163000, China*

Yibin Liu − *State Key Laboratory of Heavy Oil Processing, China University of Petroleum, Qingdao 266580, China;* orcid.org/0000-0003-2623-3868

Xiaobo Chen − *State Key Laboratory of Heavy Oil Processing, China University of Petroleum, Qingdao 266580, China;* orcid.org/0000-0001-9180-0190

De Chen − *State Key Laboratory of Heavy Oil Processing, China University of Petroleum, Qingdao 266580, China; Department of Chemical Engineering, Norwegian University of Science and Technology, Trondheim 7491, Norway*

Honghong Shan − *State Key Laboratory of Heavy Oil Processing, China University of Petroleum, Qingdao 266580, China*

Complete contact information is available at: https://pubs.acs.org/10.1021/acs.iecr.3c03543

Author Contributions

#X.D., Y.X., and J.L. contributed equally.

Notes

The authors declare no competing financial interest.

■ ACKNOWLEDGMENTS

This work was supported by the National Natural Science Foundation of China (22108305, 21978325, and 22108307), Independent Innovation Research Projects (20CX06072A, 20CX06095A, and 20CX06096A), Natural Science Foundation of Shandong Province (ZR2021QB076, ZR2020KB00, and ZR2020YQ17), and Fundamental Research Funds for the Central Universities (20CX06073A).

REFERENCES

(1) Yan, W.; Zhang, G.; Yan, H.; Liu, Y.; Chen, X.; Feng, X.; Jin, X.; Yang, C. Liquid-phase epoxidation of light olefins over W and Nb nanocatalysts. *ACS Sustainable Chem. Eng.* **2018**, *6* (4), 4423−4452.

(2) Sharma, A. S.; Sharma, V. S.; Kaur, H.; Varma, R. S. Supported heterogeneous nanocatalysts in sustainable, selective and eco-friendly epoxidation of olefins. *Green Chem.* **2020**, *22* (18), 5902−5936.

(3) Rault, I.; Frei, V.; Herbage, D.; Abdul-Malak, N.; Huc, A. Evaluation of different chemical methods for cros-linking collagen gel, films and sponges. *J. Mater. Sci. Mater. Med.* **1996**, *7* (4), 215−221.

(4) Simmons, D.; Kearney, J. Evaluation of collagen cross-linking techniques for the stabilization of tissue matrices. *Biotechnol. Appl. Biochem.* **1993**, *17* (1), 23−29.

(5) Wu, X.-W.; Li, B.-D. Preparation of high purity 1, 2-diols by catalytic oxidation of linear terminal alkenes with H_2O_2 in the presence of carboxylic acids under solvent-free conditions. *Chin. Chem. Lett.* **2014**, *25* (3), 459−462.

(6) Hoveyda, A. H.; Evans, D. A.; Fu, G. C. Substrate-directable chemical reactions. *Chem. Rev.* **1993**, *93* (4), 1307−1370.

(7) Harvey, B. G.; Meylemans, H. A. 1-Hexene: a renewable C_6 platform for full-performance jet and diesel fuels. *Green Chem.* **2014**, *16* (2), 770−776.

(8) Nijhuis, T. A.; Makkee, M.; Moulijn, J. A.; Weckhuysen, B. M. The production of propene oxide: catalytic processes and recent developments. *Ind. Eng. Chem. Res.* **2006**, *45* (10), 3447−3459.

(9) Lu, X.; Wu, H.; Jiang, J.; He, M.; Wu, P. Selective synthesis of propylene oxide through liquid-phase epoxidation of propylene with H_2O_2 over formed Ti-MWW catalyst. *J. Catal.* **2016**, *342*, 173−183.

(10) Bach, R. D.; Canepa, C.; Winter, J. E.; Blanchette, P. E. Mechanism of acid-catalyzed epoxidation of alkenes with peroxy acids. *J. Org. Chem.* **1997**, *62* (15), 5191−5197.

(11) Colladon, M.; Scarso, A.; Sgarbossa, P.; Michelin, R. A.; Strukul, G. Regioselectivity and diasteroselectivity in Pt (II)-mediated "green" catalytic epoxidation of terminal alkenes with hydrogen peroxide: Mechanistic insight into a peculiar substrate selectivity. *J. Am. Chem. Soc.* **2007**, *129* (24), 7680−7689.

(12) De Vos, D. E.; de Wildeman, S.; Sels, B. F.; Grobet, P. J.; Jacobs, P. A. Selective alkene Oxidation with H_2O_2 and a Heterogenized Mn Catalyst: epoxidation and a New Entry to Vicinal cis-Diols. *Angew. Chem. Int. Ed* **1999**, *38* (7), 980−983.

(13) Arends, I.; Sheldon, R. Recent developments in selective catalytic epoxidations with H_2O_2. *Top. Catal.* **2002**, *19*, 133−141.

(14) Peregot, G.; Bellussi, G.; Corno, C.; Taramasso, M.; Buonomot, F.; Esposito, A., Titanium-silicalite: a novel derivative in the pentasil family. In *Studies in surface science and catalysis*; Elsevier: 1986; Vol. *28*, pp 129−136.

(15) Clerici, M. G.; Kholdeeva, O. A. *Liquid phase oxidation via heterogeneous catalysis: organic synthesis and industrial applications*. John Wiley & Sons: 2013.

(16) Clerici, M.; Bellussi, G.; Romano, U. Synthesis of propylene oxide from propylene and hydrogen peroxide catalyzed by titanium silicalite. *J. Catal.* **1991**, *129* (1), 159−167.

(17) Russo, V.; Tesser, R.; Santacesaria, E.; Di Serio, M. Chemical and technical aspects of propene oxide production via hydrogen peroxide (HPPO process). *Ind. Eng. Chem. Res.* **2013**, *52* (3), 1168−1178.

(18) Corma, A.; Diaz, U.; Domine, M. E.; Fornés, V. New aluminosilicate and titanosilicate delaminated materials active for acid catalysis, and oxidation reactions using H2O2. *J. Am. Chem. Soc.* **2000**, *122* (12), 2804−2809.

(19) Zuo, Y.; Liu, M.; Zhang, T.; Hong, L.; Guo, X.; Song, C.; Chen, Y.; Zhu, P.; Jaye, C.; Fischer, D. Role of pentahedrally coordinated titanium in titanium silicalite-1 in propene epoxidation. *RSC Adv.* **2015**, *5* (23), 17897−17904.

(20) Guo, Q.; Sun, K.; Feng, Z.; Li, G.; Guo, M.; Fan, F.; Li, C. A thorough investigation of the active titanium species in TS-1 zeolite by in situ UV resonance Raman spectroscopy. *Chem. - Eur. J.* **2012**, *18* (43), 13854−13860.

(21) Su, J.; Xiong, G.; Zhou, J.; Liu, W.; Zhou, D.; Wang, G.; Wang, X.; Guo, H. Amorphous Ti species in titanium silicalite-1: Structural features, chemical properties, and inactivation with sulfosalt. *J. Catal.* **2012**, *288*, 1−7.

(22) Notari, B. Titanium silicalites. *Catal. Today* **1993**, *18* (2), 163−172.

(23) Zhuang, J.; Ma, D.; Yan, Z.; Deng, F.; Liu, X.; Han, X.; Bao, X.; Liu, X. W.; Guo, X.; Wang, X. Solid-state MAS NMR detection of the oxidation center in TS-1 zeolite by in situ probe reaction. *J. Catal.* **2004**, *221* (2), 670−673.

(24) Wells, D. H., Jr; Delgass, W. N., Jr; Thomson, K. T. Evidence of defect-promoted reactivity for epoxidation of propylene in titanosilicate (TS-1) catalysts: a DFT study. *J. Am. Chem. Soc.* **2004**, *126* (9), 2956−2962.

(25) Wang, Y.; Li, L.; Bai, R.; Gao, S.; Feng, Z.; Zhang, Q.; Yu, J. Amino acid-assisted synthesis of TS-1 zeolites containing highly catalytically active TiO_6 species. *Chin. J. Catal.* **2021**, *42* (12), 2189−2196.

(26) Wu, L.; Tang, Z.; Yu, Y.; Yao, X.; Liu, W.; Li, L.; Yan, B.; Liu, Y.; He, M. Facile synthesis of a high-performance titanosilicate catalyst with controllable defective Ti $(OSi)_3OH$ sites. *Chem. Commun.* **2018**, *54* (49), 6384−6387.

(27) Panyaburapa, W.; Nanok, T.; Limtrakul, J. epoxidation reaction of unsaturated hydrocarbons with H_2O_2 over defect TS-1 investigated by ONIOM method: formation of active sites and reaction mechanisms. *J. Phys. Chem. C* **2007**, *111* (8), 3433−3441.

(28) Ramachandran, C. E.; Du, H.; Kim, Y. J.; Kung, M. C.; Snurr, R. Q.; Broadbelt, L. J. Solvent effects in the epoxidation reaction of 1-hexene with titanium silicalite-1 catalyst. *J. Catal.* **2008**, *253* (1), 148−158.

(29) Ayla, E. Z.; Potts, D. S.; Bregante, D. T.; Flaherty, D. W. alkene epoxidations with H_2O_2 over groups 4−6 metal-substituted BEA zeolites: reactive intermediates, reaction pathways, and linear free-energy relationships. *ACS Catal.* **2021**, *11* (1), 139−154.

(30) Lin, D.; Feng, X.; Zheng, X.; Xu, Y.; Zhao, H.; Song, Z.; Wang, L.; Shan, H.; Xiao, F.; Chen, D.; Yang, C. Dimensional Regulation of Titanosilicate by Kinetically Controlled Intergrowth Crystals. *Adv. Funct. Mater.* **2023**, 2301179.

(31) Lin, D.; Zhang, Q.; Qin, Z.; Li, Q.; Feng, X.; Song, Z.; Cai, Z.; Liu, Y.; Chen, X.; Chen, D.; Mintova, S.; Yang, C. Reversing titanium oligomer formation towards high-efficiency and green synthesis of titanium-containing molecular sieves. *Angew. Chem. Int. Ed* **2021**, *60* (7), 3443−3448.

(32) Song, Z.; Feng, X.; Sheng, N.; Lin, D.; Li, Y.; Liu, Y.; Chen, X.; Chen, D.; Zhou, X.; Yang, C. Cost-efficient core-shell TS-1/silicalite-1 supported Au catalysts: Towards enhanced stability for propene epoxidation with H_2 and O_2. *Chem. Eng. J.* **2019**, *377*, 119927.

(33) Bordiga, S.; Bonino, F.; Damin, A.; Lamberti, C. Reactivity of Ti (iv) species hosted in TS-1 towards H_2O_2−H_2O solutions investigated by ab initio cluster and periodic approaches combined with experimental XANES and EXAFS data: a review and new highlights. *Phys. Chem. Chem. Phys.* **2007**, *9* (35), 4854−4878.

(34) Bellussi, G.; Millini, R.; Pérez Pariente, J.; Sánchez-Sánchez, M. Background and recent advances in Ti-containing zeolite materials. *Struct. React. Metals Zeolite Mater.* **2018**, 1−52.

(35) Berry, A. J.; Danyushevsky, L. V.; St C O'Neill, H.; Newville, M.; Sutton, S. R. Oxidation state of iron in komatiitic melt inclusions indicates hot Archaean mantle. *Nature* **2008**, *455* (7215), 960−963.

(36) Liu, C.; Huang, J.; Sun, D.; Zhou, Y.; Jing, X.; Du, M.; Wang, H.; Li, Q. anatase type extra-framework titanium in TS-1: A vital factor influencing the catalytic activity toward styrene epoxidation. *Appl. Catal. A-Gen* **2013**, *459*, 1−7.

(37) Přech, J.; Vitvarová, D.; Lupínková, L.; Kubů, M.; Čejka, J. Titanium impregnated borosilicate zeolites for epoxidation catalysis. *Microporous Mesoporous Mater.* **2015**, *212*, 28−34.

(38) Ma, H.; Lin, H.; Liu, X.; Lü, H.; Zhu, Z. In situ structural reconstruction triggers the hydrothermal synthesis of hierarchical Ti-Beta zeolites for oxidative desulfurization. *Mater. Chem. Front.* **2021**, *5* (16), 6101−6113.

https://doi.org/10.1021/acs.iecr.3c03543
Ind. Eng. Chem. Res. XXXX, XXX, XXX−XXX

(39) Ren, W.; Hua, Z.; Ge, T.; Zhou, X.; Chen, L.; Zhu, Y.; Shi, J. Post-synthesis of hierarchically structured Ti-β zeolites and their epoxidation catalytic performance. *Chin. J. Catal.* **2015**, *36* (6), 906−912.
(40) Omegna, A.; Vasic, M.; Anton van Bokhoven, J.; Pirngruber, G.; Prins, R. dealumination and realumination of microcrystalline zeolite beta: an XRD, FTIR and quantitative multinuclear (MQ) MAS NMR study. *Phys. Chem. Chem. Phys.* **2004**, *6* (2), 447−452.
(41) Carati, A.; Flego, C.; Previde Massara, E.; Millini, R.; Carluccio, L.; Parker, W. O.; Bellussi, G. Stability of Ti in MFI and Beta structures: a comparative study. *Microporous Mesoporous Mater.* **1999**, *30* (1), 137−144.
(42) Hoeven, N.; Mali, G.; Mertens, M.; Cool, P. Design of Ti-Beta zeolites with high Ti loading and tuning of their hydrophobic/hydrophilic character. *Microporous Mesoporous Mater.* **2019**, *288*, No. 109588.
(43) Ikuno, T.; Chaikittisilp, W.; Liu, Z.; Iida, T.; Yanaba, Y.; Yoshikawa, T.; Kohara, S.; Wakihara, T.; Okubo, T. Structure-directing behaviors of tetraethylammonium cations toward zeolite beta revealed by the evolution of aluminosilicate species formed during the crystallization process. *J. Am. Chem. Soc.* **2015**, *137* (45), 14533−14544.
(44) Zhang, Z.; Zhao, X.; Wang, G.; Xu, J.; Lu, M.; Tang, Y.; Fu, W.; Duan, X.; Qian, G.; Chen, D.; Zhou, X. Uncalcined TS-2 immobilized Au nanoparticles as a bifunctional catalyst to boost direct propylene epoxidation with H_2 and O_2. *AIChE J.* **2020**, *66* (2), No. e16815.
(45) Corma, A.; García, H. Lewis acids as catalysts in oxidation reactions: from homogeneous to heterogeneous systems. *Chem. Rev.* **2002**, *102* (10), 3837−3892.
(46) Hunger, B.; Heuchel, M.; Clark, L. A.; Snurr, R. Q. Characterization of acidic OH groups in zeolites of different types: An interpretation of NH_3-TPD results in the light of confinement effects. *J. Phys. Chem. B* **2002**, *106* (15), 3882−3889.
(47) Xiong, G.; Cao, Y.; Guo, Z.; Jia, Q.; Tian, F.; Liu, L. The roles of different titanium species in TS-1 zeolite in propylene epoxidation studied by in situ UV Raman spectroscopy. *Phys. Chem. Chem. Phys.* **2016**, *18* (1), 190−196.
(48) Tang, Z.; Yu, Y.; Liu, W.; Chen, Z.; Wang, R.; Liu, H.; Wu, H.; Liu, Y.; He, M. Deboronation-assisted construction of defective $Ti(OSi)_3OH$ species in MWW-type titanosilicate and their enhanced catalytic performance. *Catal. Sci. Technol.* **2020**, *10* (9), 2905−2915.
(49) Grosso-Giordano, N. A.; Hoffman, A. S.; Boubnov, A.; Small, D. W.; Bare, S. R.; Zones, S. I.; Katz, A. Dynamic reorganization and confinement of TiIV active sites controls olefin epoxidation catalysis on two-dimensional zeotypes. *J. Am. Chem. Soc.* **2019**, *141* (17), 7090−7106.
(50) Li, P.; Liu, G.; Wu, H.; Liu, Y.; Jiang, J.-g.; Wu, P. Postsynthesis and selective oxidation properties of nanosized Sn-Beta zeolite. *J. Phys. Chem. C* **2011**, *115* (9), 3663−3670.
(51) Shamzhy, M.; Přech, J.; Zhang, J.; Ruaux, V.; El-Siblani, H.; Mintova, S. Quantification of Lewis acid sites in 3D and 2D TS-1 zeolites: FTIR spectroscopic study. *Catal. Today* **2020**, *345*, 80−87.
(52) Wu, L.; Deng, X.; Zhao, S.; Yin, H.; Zhuo, Z.; Fang, X.; Liu, Y.; He, M. Synthesis of a highly active oxidation catalyst with improved distribution of titanium coordination states. *Chem. Commun.* **2016**, *52* (56), 8679−8682.
(53) Lin, W.; Frei, H. Photochemical and FT-IR probing of the active site of hydrogen peroxide in Ti silicalite sieve. *J. Am. Chem. Soc.* **2002**, *124* (31), 9292−9298.
(54) Wang, L.; Sun, J.; Meng, X.; Zhang, W.; Zhang, J.; Pan, S.; Shen, Z.; Xiao, F.-S. A significant enhancement of catalytic activities in oxidation with H_2O_2 over the TS-1 zeolite by adjusting the catalyst wettability. *Chem. Commun.* **2014**, *50* (16), 2012−2014.
(55) Laha, S.; Kumar, R. Selective epoxidation of styrene to styrene oxide over TS-1 using urea−hydrogen peroxide as oxidizing agent. *J. Catal.* **2001**, *204* (1), 64−70.
(56) Fan, W.; Wu, P.; Tatsumi, T. Unique solvent effect of microporous crystalline titanosilicates in the oxidation of 1-hexene and cyclohexene. *J. Catal.* **2008**, *256* (1), 62−73.
(57) Guo, S.; Zhang, Y.; Ye, Y.; Song, J.; Li, M. MWW-type titanosilicate synthesized by simply treating ERB-P zeolite with acidic H_2TiF_6 and its catalytic performance in a liquid epoxidation of 1-hexene with H_2O_2. *ACS Omega* **2020**, *5* (17), 9912−9919.
(58) Song, X.; Yang, X.; Zhang, T.; Zhang, H.; Zhang, Q.; Hu, D.; Chang, X.; Li, Y.; Chen, Z.; Jia, M.; Zhang, P.; Yu, J. Controlling the morphology and titanium coordination states of TS-1 zeolites by crystal growth modifier. *Inorg. Chem.* **2020**, *59* (18), 13201−13210.
(59) Zhang, T.; Chen, X.; Chen, G.; Chen, M.; Bai, R.; Jia, M.; Yu, J. Synthesis of anatase-free nano-sized hierarchical TS-1 zeolites and their excellent catalytic performance in alkene epoxidation. *J. Mater. Chem.* **2018**, *6* (20), 9473−9479.
(60) Xu, W.; Zhang, T.; Bai, R.; Zhang, P.; Yu, J. A one-step rapid synthesis of TS-1 zeolites with highly catalytically active mononuclear TiO_6 species. *J. Mater. Chem.* **2020**, *8* (19), 9677−9683.
(61) Zhang, Z.; Shi, S.; Tang, Y.; Xu, J.; Du, W.; Wang, Q.; Yu, D.; Liao, Y.; Song, N.; Duan, X.; Zhou, X. Using ammonia solution to fabricate highly active Au/uncalcined TS-1 catalyst for gas-phase epoxidation of propylene. *J. Catal.* **2022**, *416*, 410−422.
(62) Tozzola, G.; Mantegazza, M. A.; Ranghino, G.; Petrini, G.; Bordiga, S.; Ricchiardi, G.; Lamberti, C.; Zulian, R.; Zecchina, A. On the Structure of the Active Site of Ti-Silicalite in Reactions with Hydrogen Peroxide: A Vibrational and Computational Study. *J. Catal.* **1998**, *179* (1), 64−71.
(63) Bonino, F.; Damin, A.; Ricchiardi, G.; Ricci, M.; Spanò, G.; D'Aloisio, R.; Zecchina, A.; Lamberti, C.; Prestipino, C.; Bordiga, S. Ti-peroxo species in the TS-1/H_2O_2/H_2O system. *J. Phys. Chem. B* **2004**, *108* (11), 3573−3583.
(64) Bregante, D. T.; Thornburg, N. E.; Notestein, J. M.; Flaherty, D. W. Consequences of Confinement for alkene epoxidation with Hydrogen Peroxide on Highly Dispersed Group 4 and 5 Metal Oxide Catalysts. *ACS Catal.* **2018**, *8* (4), 2995−3010.
(65) Ayla, E. Z.; Potts, D. S.; Bregante, D. T.; Flaherty, D. W. alkene epoxidations with H_2O_2 over Groups 4−6 Metal-Substituted BEA Zeolites: Reactive Intermediates, Reaction Pathways, and Linear Free-Energy Relationships. *ACS Catal.* **2021**, *11* (1), 139−154.
(66) Bordiga, S.; Damin, A.; Bonino, F.; Ricchiardi, G.; Lamberti, C.; Zecchina, A. The structure of the peroxo species in the TS-1 catalyst as investigated by resonant Raman spectroscopy. *Angew. Chem., Int. Ed. Engl.* **2002**, *41* (24), 4734−7.
(67) Yoon, C. W.; Hirsekorn, K. F.; Neidig, M. L.; Yang, X.; Tilley, T. D. Mechanism of the decomposition of aqueous hydrogen peroxide over heterogeneous TiSBA15 and TS-1 selective oxidation catalysts: insights from spectroscopic and density functional theory studies. *ACS Catal.* **2011**, *1* (12), 1665−1678.
(68) Lin, D.; Xu, Y.; Zheng, X.; Sheng, W.; Liu, Z.; Yan, Y.; Cao, Y.; Liu, Y.; Feng, X.; Chen, D. Engineering Sodium-decorated Bifunctional Au-Ti Sites to Boost Molecular Transfer for propene epoxidation with H_2 and O_2. *AIChE J.* **2023**, No. e17999.
(69) Liang, X.; Peng, X.; Liu, D.; Xia, C.; Luo, Y.; Shu, X. Understanding the mechanism of N coordination on framework Ti of Ti-BEA zeolite and its promoting effect on alkene epoxidation reaction. *Mol. Catal.* **2021**, *511*, No. 111750.
(70) Nie, X.; Ji, X.; Chen, Y.; Guo, X.; Song, C. Mechanistic investigation of propylene epoxidation with H_2O_2 over TS-1: Active site formation, intermediate identification, and oxygen transfer pathway. *Mol. Catal.* **2017**, *441*, 150−167.
(71) Xu, L.; Huang, D. D.; Li, C. G.; Ji, X.; Jin, S.; Feng, Z.; Xia, F.; Li, X.; Fan, F.; Li, C.; Wu, P. Construction of unique six-coordinated titanium species with an organic amine ligand in titanosilicate and their unprecedented high efficiency for alkene epoxidation. *Chem. Commun.* **2015**, *51* (43), 9010−9013.

https://doi.org/10.1021/acs.iecr.3c03543
Ind. Eng. Chem. Res. XXXX, XXX, XXX−XXX